The hydrogen interaction in an FCC FePd alloy with a vacancy

2009 Phys. Scr. 79 045702

(http://iopscience.iop.org/1402-4896/79/4/045702)

Phys. Scr. **79** (2009) 045702 (5pp) doi:10.1088/0031-8949/79/04/045702

The hydrogen interaction in an FCC FePd alloy with a vacancy

S Ardenghi[1], E González[2], P Jasen[2] and A Juan[2]

[1] Instituto de Astronomía y Física del Espacio (IAFE), CC 67—Suc 28 (C1428ZAA) Ciudad Autónoma de Buenos Aires, Argentina
[2] Departamento de Física, Universidad Nacional del Sur, Av. Alem 1253 Bahía Blanca (8000), Argentina

E-mail: cajuan@uns.edu.ar

Received 30 September 2008
Accepted for publication 4 February 2009
Published 31 March 2009
Online at stacks.iop.org/PhysScr/79/045702

Abstract
The absorption of hydrogen in the ordered face-centered cubic FePd alloy is investigated using a density functional calculation method. Changes in the electronic structure and bonding after introducing an Fe or Pd vacancy are analysed. H locates close to a tetrahedral site and the H–metal bond is achieved at the expense of the interfacial Fe–Pd bond.

PACS numbers: 71.20b, 71.55Ak

1. Introduction

FePd alloys are interesting for several reasons: first, Fe and Pd have different structures in their elemental phases while they form a single unique lattice upon alloying; second, they exhibit Invar characteristics around the 3 : 1 stoichiometric composition; third, recent studies have identified the system as a potential candidate for magnetic media and shape memory applications due to strong magnetic anisotropy [1–5]. There have been experimental investigations on the lattice dynamics and its coupling with magnetic ordering in disordered phases [6, 7], on the lattice dynamics in intermetallics $FePd_3$ [8] and FePd [9], and on estimation of vacancy formation enthalpy and migration enthalpy [10], which govern the diffusion and ordering kinetics.

FePd alloy exhibits a phase transition between the disordered face-centered cubic (FCC) phase and the $L1_0$ (CuAu(I) type) ordered tetragonal structure around 920 K at the equiatomic composition [11]. The ordered structure is based on the FCC lattice and consists of alternating planes of Fe and Pd atoms. This very anisotropic chemical ordering leads to a small tetragonality of the lattice ($c/a \approx 0.94$) and to both mechanical and magnetic anisotropies.

The Fe and Pd atoms form at high temperatures (>1000 K) a continuous FCC solid solution (γ FePd with Fm3m space group). At Pd concentrations >60 at %, an ordering transformation of this disordered phase to an $L1_2$ phase (γ_2 with Pm3m space group and Cu_3Au prototype) is observed when temperature is reduced [12–14].

The vacancy is one of the simplest defects in crystal structure and so represents a benchmark for experimental and theoretical understanding. When a vacancy is formed, the surrounding material reacts both electronically and elastically [15].

Vacancy migration is the dominant mechanism behind atomic transport, i.e., self-diffusion, in most elemental crystals, and is of fundamental importance in processes like solid phase transformations, nucleation and defect migration [15, 16]. Vacancies also play an important role for surface morphology, as shown very recently [17].

Metals can absorb hydrogen atoms during manufacture and/or service. These dissolved hydrogen atoms can greatly affect the mechanical properties of structural metals, often leading to material failure. In particular, hydrogen frequently decreases a metal's ductility (hydrogen embrittlement (HE)) [18]. HE occurs in both polycrystalline and single-crystal samples of pure metals and alloys [19–24].

The effects of hydrogen on vacancy properties in metals have received considerable attention in scientific and technological fields. Large volume contraction under high hydrogen pressure was found in some metals, including alpha-Fe [25, 26]. This universal phenomenon was explained by an idea of superabundant vacancy formation induced by hydrogen. Enhancement of interdiffusion at the junction of two metals [27] was attributed to the difference of the hydrogen-enhanced stabilization of vacancies. A superlattice of hydrogen–vacancy complexes (V_mH_n) was observed in the x-ray analysis [28].

Tensile experiments with hydrogen-charged samples showed that the susceptibility of steel to HE increases with the number of strong trap sites for solute hydrogen

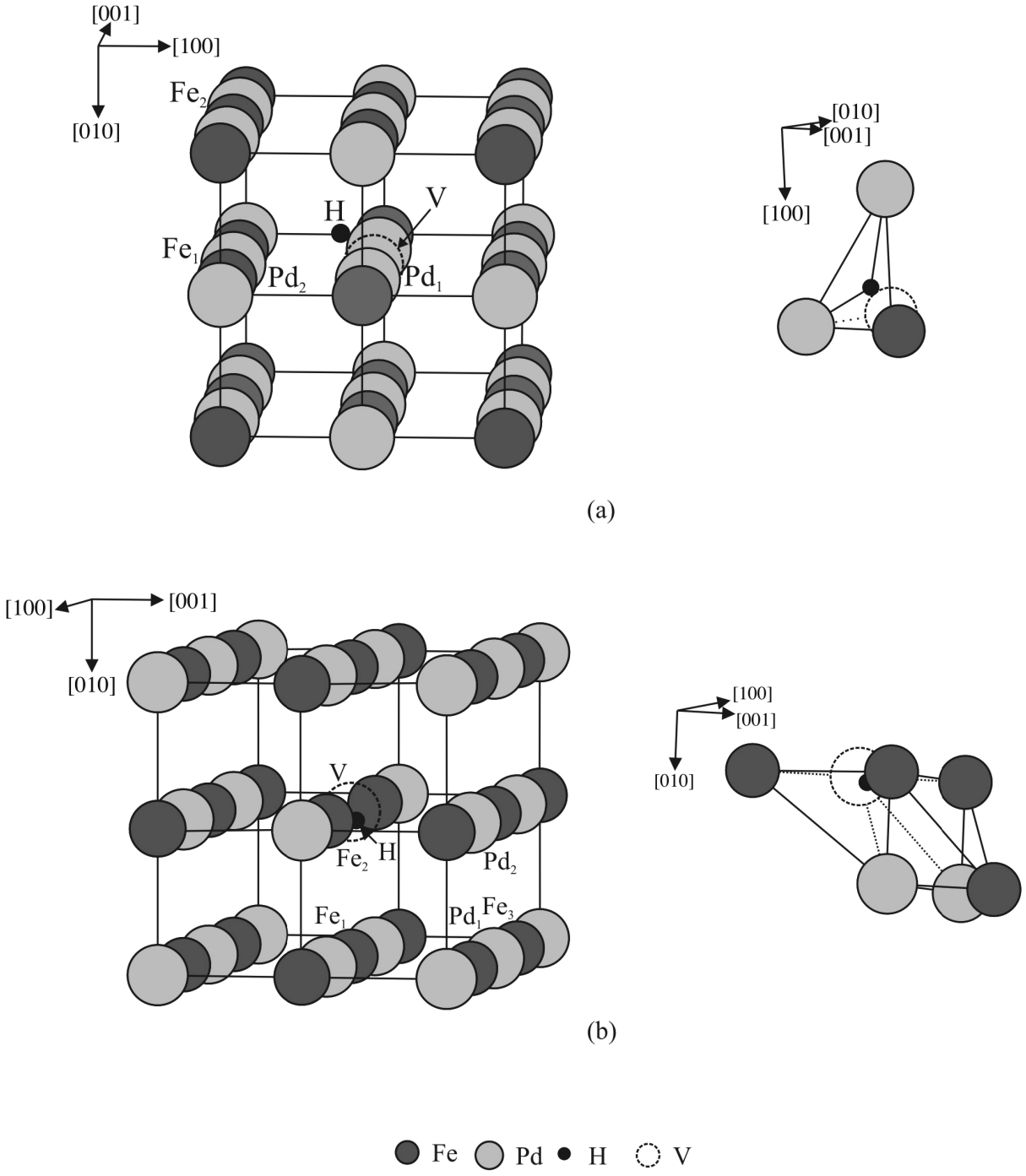

Figure 1. Schematic view of the FCC FePd + V alloy showing final location for H. Fe vacancy (a) and Pd vacancy (b). The geometrical environment of metallic atoms surrounding the H is shown at right. The metal vacancy is indicated with a dotted line.

[29 and reference therein, 30]. It was then suggested that those sites correspond to some point defects like vacancies [31]. However, no clear (quantitative) characterization has been provided on the defects states and their interactions with hydrogen.

The objectives of this paper are to study at a theoretical level the H–vacancy interaction in an FePd alloy.

2. Computational method

Gradient-corrected density functional theory (GC-DFT) calculations were performed on a supercell containing 125 atomic sites in an FCC lattice to model bulk FePd, with a $4 \times 4 \times 4$ reciprocal space grid in the supercell Brillouin zone (BZ) and a plane-wave kinetic energy cutoff of 250 eV for the Fe–Pd–H system [32–34].

We used a periodic DFT (ADF-BAND) [35]. The molecular orbitals were represented as linear combinations of Slater functions. The gradient correction Becke [36] approximation for the exchange energy functional and the B3LYP [37] approximation for the correlation functional were employed. To increase computational efficiency, the innermost atomic shells of electrons are kept frozen for every atom except hydrogen, since the internal electrons do not contribute significantly to the bonding.

Table 1. Electron density, overlap population, charge and distances for FePd FCC perfect alloy, the alloy with the vacancy and the alloy + V after H adsorption.

Structure	Electronic occupation			Charge	Bond type	OP	Distances (Å)
	s	p	d				
FePd							
Fe	0.56	0.06	5.08	2.419	Fe–Fe	0.015	2.758
Pd	0.78	0.85	8.95	−0.583	Pd–Pd	0.025	2.758
					Fe–Pd	0.362	1.950
FePd + V_{Fe}							
Fe	0.56	0.05	5.23	2.255	Fe–Fe	0.010	2.758
Pd	0.78	0.85	9.11	−0.738	Pd–Pd	0.065	2.758
					Fe–Pd	0.385	1.950
FePd + V_{Fe} + H							
H	1.22	0.00	0.00	−0.224			
Fe	0.53	0.08	5.09	2.460	Fe–Fe	0.004	2.758
Pd	0.71	0.86	9.04	−0.616	Pd–Pd	0.018	2.758
					Fe–Pd	0.324	1.950
					Fe–H	0.032	2.128
					Pd–H	0.388	1.557
FePd + V_{Pd}							
Fe	0.59	0.01	4.77	1.928	Fe–Fe	0.062	2.758
Pd	0.78	0.87	8.86	−0.510	Pd–Pd	0.026	2.758
					Fe–Pd	0.412	1.950
FePd + V_{Pd} + H							
Fe	0.53	0.08	5.09	2.460	Fe–Fe	0.023	2.758
Pd	0.71	0.86	9.04	−0.616	Pd–Pd	0.024	2.758
					Fe–Pd	0.396	1.950
H	1.32	0.00	0.00	−0.319	Fe–H	0.196	1.829
					Pd–H	0.007	2.599

We used a triple-zeta basis set (this means three Slater-type functions for each atomic valence orbital occupied) with polarization functions to express the atomic orbitals of Fe and Pd. The accurate quadratic tetrahedron procedure [38] was used for BZ integrations, and integration parameters were chosen to achieve convergence well within 50 meV.

Geometry was optimized until changes in the energy gradient and in the Cartesian coordinates were 0.001 Hartree Å and 0.01 Å, respectively. Only the Fe or Pd atom's first neighbours to the vacancy were allowed to relax. After finding the most stable position for impurities in the zone near the vacancy, we studied the Fe–H and the Pd–H interactions.

To understand the Fe–Pd–H interactions, we used the concept of density of states (DOS) and overlap population DOS (OPDOS) [39, 40].

Absorption energy was computed as the difference ΔE between the Fe–Pd–H composite system when the H atom is absorbed in its minimum energy geometry and when it is far away from the Fe–Pd alloy. It can be expressed as

$$\Delta E_{\text{Total}} = E(\text{FePdH}) - (E(\text{FePd}) + \text{E(H)}),$$

where E is the electronic energy, E(FePd) corresponds to the pure surface alloy and E(H) is the hydrogen 1 s ionization energy, near the vacancy site.

3. Model of the FePd FCC alloy with a vacancy

We studied the H absorption on the FCC FePd phase alloy structure using a supercell of 124 + V(vacancy) atoms, distributed in seven layers of the (001) plane. The high-temperature phase has an FCC crystal structure that has a well-known NaCl-type structure with a lattice parameter $a_0 = 3.90$ Å (see figure 1(a)) [41].

The structure has two types of interstitial sites, one tetrahedral (T) and one octahedral (O). All the interstitial sites (T or O) are equivalent with the same chemical environment around the site. We have introduced separately two types of vacancies Fe or Pd placed exactly at the centre of the supercell (unit cell).

To study the absorption of H, we mapped the energy surfaces with 0.01 Å steps in the central region of the cluster with cuts perpendicular to the (001) planes. After determining the more stable position for the impurity atom, we have studied the electronic interaction between this interstitial and the metallic atoms.

4. Results and discussions

Let us first discuss the electronic structure of pure and perfect FePd alloy. In the total DOS for FePd FCC, the bandwidth is 8.5 eV and Pd-based states are much less dispersed (≈4.5 eV). The Pd result negatively charged with respect to the Fe atoms.

Regarding the bonding, the OPDOS curves are almost all bonding for Fe, except near the Fermi level (E_F). For Pd–Pd, the first half of OPDOS is metal–metal bonding and the second part (closer to the E_F) antibonding.

The Fe–Pd interfacial bond OP value is much higher than that of Fe–Fe or Pd–Pd bonds. When an Fe vacancy (V_{Fe}) is introduced the Fe–Fe OP increases from 0.015 to 0.062, while the Fe–Pd OP increases 13.8%. The Pd–Pd OP bond increases

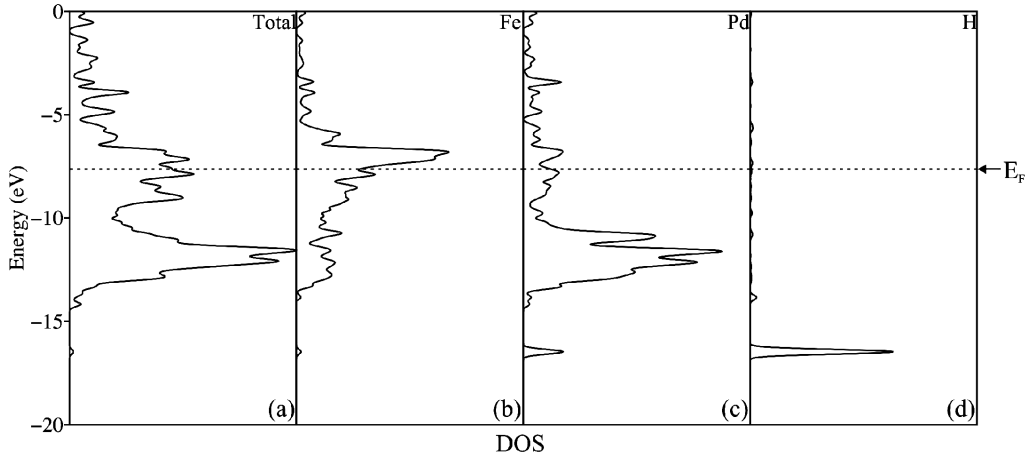

Figure 2. DOS curves for the FePd alloy with a Fe vacancy after H absorption. Total DOS (a), projected on a Fe atom (b), on a Pd atom (c) and on H atom.

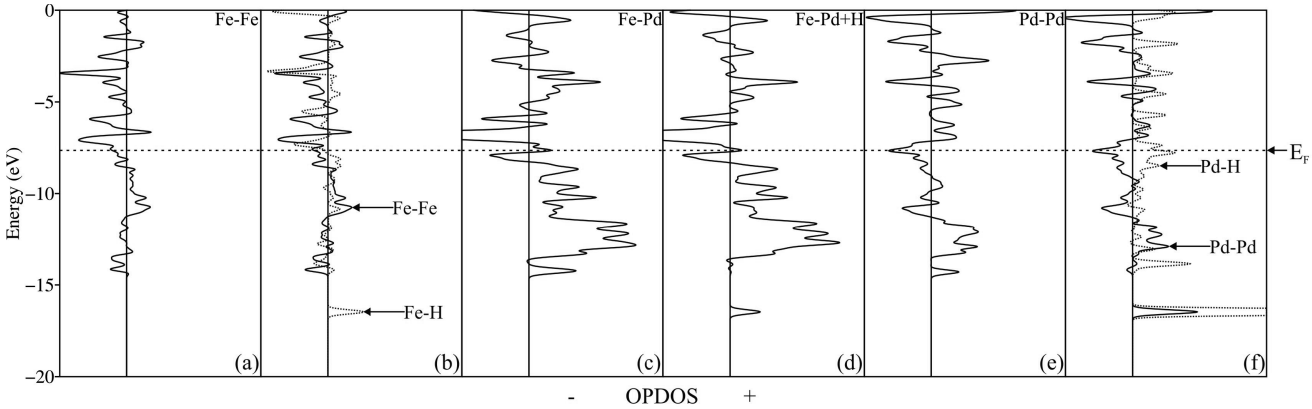

Figure 3. OPDOS curves for the FePd + Fe_V alloy before (left) and after (right) H absorption. Fe–Fe (a), Fe–Fe and Fe–H (b), Fe–Pd (c) Fe–Pd (d), Pd–Pd (e) and Pd–Pd and Pd–H (f) bonding.

by 160%. This is a typical effect that occurs when the orbitals close to E_F are antibonding, and this has been discussed in detail by Juan and Hoffman [42]. In the case of a Pd vacancy (V_{Pd}), this effect is not relevant in Pd–Pd because its states are much less antibonding than the Fe–Fe states. In table 1, the valence orbital populations, electron density, charges and overlap populations are summarized.

The DOS plots for the V_{Pd} situation (not shown here) present contributions at the bottom of the d band by narrow Pd-based states and the top of the band is formed by the Fe-based states.

The hydrogen absorption in FePd + V alloy is a favourable process. The introduction of an Fe vacancy produced a much more favourable situation when compared with the Pd vacancy. The relationship of the H-stability is four times in favour of the V_{Fe} alloy. In this case, H locates in a quasi-tetrahedral site (see figure 1(a)). When a Pd vacancy is considered, H finally resides in between a tetra- and an octahedral site (see figure 1(b)). The H-site (T or O) distance is similar in both cases and about 1.43 Å.

Table 1 presents the Fe–H and the Pd–H equilibrium distances for V_{Fe} or V_{Pd} alloy. The Fe–H distance in the case of V_{Pd} is close to the measured value for H adsorption on Fe(111) and Fe–H mono-hydrides [43]. The Pd–H distance (when a V_{Fe} is considered) is 1.56 Å and is smaller than that obtained for interstitial H in the FePd perfect alloy [44]. We have obtained the same Pd–H distance as that in the top position on Pd(001) determined by Tománek *et al* [45] and Paul and Sautet [46] using *ab initio* calculation, and reported by Efremenko in a recent review [47]. The electronic similarities between inner vacancies and free surfaces were discussed by Juan and Hoffmann [42].

The DOS plots in figure 2 show a small peak at −16.6 eV corresponding to H-based states stabilized after absorption. The curve for V_{Pd} is similar.

There are electron transfers of 0.22e- (V_{Fe}) and −0.32 (V_{Pd}), in both cases coming from the metals to H. When H is present, all OPs between metals decrease. The Pd–Pd OP decreases 72.3%, the Fe–Fe 60.0% and the interfacial bond 15.8% for a V_{Fe}. In the case of V_{Pd}, the OP also decreases but the effect seems to be moderate for the intermetallic bond (Fe–Fe 62.9%, Pd–Pd 7.7% and Fe–Pd 3.9%).

The OPDOS curves in figure 3(b) (Fe_V) for Fe–H (or Pd–H in the case of V_{Pd}) bond shows a small bonding contribution. The Fe–Pd or Pd–Pd bonding area in the OPDOS curves decreases when H is present (compare figure 3(c) vs. 3(d) and 3(e) vs. 3(f)). The OPDOS Pd–H curve is all bonding and is much higher than the Fe–H bond.

The present calculation allows us to predict the preferable site location of H close to an Fe or Pd vacancy. The H bonds mainly to Pd atoms when an Fe vacancy is considered [44]. We found some similarities with the H adsorption on Pd or

Fe surfaces. Our results are in good agreement with related *ab initio* calculations [45–47].

Acknowledgments

Our work was supported by SGCyT Universidad Nacional del Sur, PICT 655/2006 and 560/2007. A Juan, E Gonzalez and P Jasen are members of CONICET. S Ardenghi is a fellow of that institution.

References

[1] Gehanno V, Marty A, Gilles B and Samson Y 1997 *Phys. Rev.* B **55** 12552
[2] Kamp P *et al* 1999 *Phys. Rev.* B **59** 1105
[3] Bernas H, Attané J-Ph, Heinig K-H, Halley D, Ravelosona D, Marty A, Auric P, Chappert C and Samson Y 2003 *Phys. Rev. Lett.* **91** 077203
[4] Tanaka K, Ichitsubo T and Koiwa M 2001 *Mater. Sci. Eng.* A **312** 118
Morioka K and Tanaka K 2001 *Proc. Fourth Pacific Rim Int. Conf. on Advanced Materials and Processing (PRICM4), Japan Institute of Metals* ed S Hanada, Z Zhong, S W Nam and R N Wright
[5] Tanaka K, Ichitsubo T and Koiwa M 2001 *Mater. Sci. Eng.* A **312** 118
[6] Maliszewski E, Sosnowski J, Bednarski S, Czachor A and Holas A 1975 *J. Phys. F: Met. Phys.* **5** 1455
[7] Sato M, Grier B H, Shapiro S M and Miyajima H 1982 *J. Phys. F: Met. Phys.* **12** 2117
[8] Stirling W G, Cowley R A and Stringfellow M W 1972 *J. Phys. F: Met. Phys.* **2** 421
[9] Ghosh S 2008 *J. Phys.: Condens. Matter* **20** 275208
[10] Mehaddene T, Kentzinger E, Hennion B, Tanaka K, Numakura H, Marty A, Parasote V, Cadeville M C, Zemirli M and Pierron-Bohnes V 2004 *Phys. Rev.* B **69** 024304
[11] Kubachewaki O 1982 *Iron Binary Phase Diagrams* (New York: Springer)
[12] Hansen M and Anderko K 1985 *Constitution of Binary Alloys* (New York: MacGraw-Hill) p 696
[13] Peerez-Landazábal J I, Gómez-Polo C, Recarte V, Vergara J, Ortega R J and Madurga V 1999 *J. Magn. Magn. Mater.* **196–197** 179
[14] Haasen P 1996 *Physical Metallurgy* (London: Cambridge University Press)
[15] Kauffman R P and Rappe A M 2003 *Phys. Rev.* B **67** 085403
[16] Kittel C 1996 *Introduction to Solid State Physics* 7th edn (New York: Wiley)
[17] McCarty K F, Nobel J A and Bartelt N C 2001 *Nature* **412** 622
[18] Jiang D E and Carter E A 2004 *Acta Mater.* **52** 4801
[19] Oriani R A, Hirth J P and Smialoski M 1985 *Hydrogen Degradation of Ferrous Alloys* (Westwood, NJ: Noyes Publications) pp 199–212
[20] Wang J-S 2001 *Eng. Fract. Mech.* **68** 647
[21] Wang J-S 2001 *Solid Mech. Appl.* **84** 31
[22] McMahon J C J 1990 *Innovations in Ultrahigh-Strength Steels, Proc. 34th Sagamore Army Materials Research Conf.* ed G B Olson, M Azrin and E S Wright (Washington, DC: Government Printing Office) p 597
[23] Jiang D E and Carter E A 2004 *Phys. Rev.* B **70** 064102
[24] Nordlandert P, Norskov J K and Besenbacherg F 1986 *J. Phys. F: Met. Phys.* **16** 1161
[25] Fukai Y and Okuma N 1993 *Japan. J. Appl. Phys.* Part 2 **32** L1256
[26] Iwamoto M and Fukai Y 1999 *Mater. Trans. JIM* **40** 606
[27] Hayashi E, Kurokawa Y and Fukai Y 1998 *Phys. Rev. Lett.* **80** 5588
[28] Fukai Y and Okuma N 1994 *Phys. Rev. Lett.* **73** 1640
[29] Nagumo M 2001 *ISIJ Int.* **41** 590
[30] Nagumo M, Nakamura M and Takai K 2001 *Metall. Mater. Trans.* A **32** 339
[31] Nagumo M, Ohta K and Saitoh H 1999 *Scr. Mater.* **40** 313
[32] Hohenberg P and Kohn W 1964 *Phys. Rev.* **136** 864
[33] Koh W and Sham L J 1965 *Phys. Rev.* **140** 1133
[34] Parr R G and Yang W 1989 *Density Functional Theory of Atoms and Molecules* (New York: Oxford University Press)
[35] *Amsterdam Density Functional Package Release* 2001 (Amsterdam: Vrije Universiteit)
[36] Becke D 1988 *Phys. Rev.* A **38** 3098
[37] Lee C, Yang W and Parr G R 1988 *Phys. Rev.* B **37** 785
[38] Wiesenekker G, te Velde G and Baerends E J 1988 *J. Phys. C: Solid State Phys.* **21** 4263
[39] Hoffmann R 1988 *Solids and Surfaces: A Chemist's View of Bonding in Extended Structures* (New York: VCH)
[40] Landrum G and Glassey W 2001 *Yet Another Extended Hückel Molecular Orbital Package (YAeHMOP), Cornell University* YAeHMOP is freely available on the World Wide Web at http://overlap.chem.cornell.edu:8080/yahemop.html
[41] Villars P and Calvert L D 1991 *Pearson's Handbook of Crystallographic Data to Intermetallic Phases* 2nd edn (Metals Park, OH: ASM)
[42] Juan A and Hoffman R 1999 *Surf. Sci.* **421** 1
[43] Moritz W, Imbihl R, Behm R J, Ertl G and Matsushima T 1985 *J. Chem. Phys.* **83** 1959
[44] González E A, Jasen P V, Castellani N J and Juan A 2004 *J. Phys. Chem. Solids* **65** 1799
[45] Tománek D, Sun Z and Louie S G 1991 *Phys. Rev.* B **43** 4699
[46] Paul J-F and Sautet P 1996 *Phys. Rev.* B **53** 8015
[47] Efremenko I 2001 *J. Mol. Cat. A: Chem.* **173** 19